Gypsum Nucleation into Sodium Chloride Solutions

Marina Prisciandaro
Dipt. di Chimica, Ingegneria Chimica e Materiali, Università dell'Aquila, 67040 L'Aquila, Italy

Amedeo Lancia
Dipt. di Ingegneria Chimica, Università di Napoli ''Federico II,'' 80125 Napoli, Italy

Dino Musmarra
Istituto di Ricerche sulla Combustione, CNR, 80125 Napoli, Italy

The nucleation of gypsum into a NaCl solution was studied within a supersaturation range of 2−4 at 25-70°C. The experiments were carried out using a lab-scale apparatus consisting of a batch crystallizer with the related measurement devices. Signals of scattered and transmitted light coming from a He−Ne laser source were analyzed to measure the induction period, that is, the time delay necessary for homogeneous nucleation to take place. Comparison of the experimental results with those previously obtained in the absence of added NaCl in solution showed that NaCl strongly affects gypsum precipitation. They were compared in terms of the activation energy and the interfacial tension between crystals and the surrounding aqueous solution.

Introduction

The precipitation of calcium sulfate dihydrate represents an important issue in a number of different industrial applications, and for this reason a great deal of attention has been given in the literature to the study of gypsum crystal nucleation and growth, with both a fundamental and an operating approach. Several authors devoted their researches to understanding the gypsum crystallization phenomena involved in nucleation and growth processes, and to the estimation of significant parameters such as activation energy (E_{att}) and interfacial tension (γ_s) (He et al., 1994; Nielsen, 1964; Lancia et al., 1999). On the other hand, the study of the practical application of gypsum precipitation covers different fields, for example, the wet limestone−gypsum scrubbing process, for which the evaluation of the best conditions for carrying out the precipitation step focuses mainly on how to reduce the byproduct water content, making sludge disposal less expensive (Etherton and Randolph, 1981); several scale control applications, such as desalination and industrial water treatment, for which many researchers have tested the capability of disparate additives of retarding the unwanted gypsum precipitation process (Öner et al., 1998).

In a previous article (Lancia et al., 1999) this research group had devised a new method, based on a laser light scattering technique, for measuring nucleation induction period (t_{ind}), that is, the time delay necessary for homogeneous nucleation to take place. More precisely, the induction period (or induction time) is defined as the time elapsed between the onset of supersaturation and the first changes in the system's physical properties due to the formation of a solid phase (Söhnel and Garside, 1992). In fact, the true induction period (t^*, with $t^* \leq t_{\text{ind}}$), as pointed out by Söhnel and Mullin (1978), cannot be experimentally measured, since it refers to the detection of critical nuclei (or *embryos*, such as clusters of loosely aggregated molecules); in order to perform the measurement, however, it is necessary that such nuclei grow until they reach a detectable size. The only possible determination is therefore simply referred to as the induction period, which depends on the technique employed to measure it. Nevertheless, the knowledge of t_{ind} and of its relationships with the process parameters, such as the temperature and the supersaturation, can give some important information about the crystallization process (Söhnel and Mullin, 1988); obviously, the more accurate the technique, the more reliable the information obtained. A detailed review of the effect of organic

---

Correspondence concerning this article should be addressed to A. Lancia.

and inorganic additives on the induction period for gypsum nucleation was presented elsewhere (Prisciandaro et al., 1999). Analyses in the literature showed that most of the articles (Liu and Nancollas, 1975; Amjad and Hooley, 1986) concerned the effects that specific additives have on the growth kinetics of gypsum crystals, especially from seeded solutions (such as with a secondary nucleation mechanism), while a much smaller number of articles (He et al., 1994) have been published on the effect of additives on the primary nucleation kinetics of gypsum, and therefore on induction time. Moreover the only article concerning the effect of dissolved impurities on the induction period for gypsum nucleation in conditions typical of a flue-gas desulfurization process is that by Lancia et al. (1999), in which by applying the optical technique just reported, the authors measured the induction period for gypsum nucleation as a function of temperature and supersaturation. They evaluated the interfacial tension between $CaSO_4 \cdot 2H_2O$ and the surrounding aqueous solution by using the dependence of t_{ind} on supersaturation, while the dependence of t_{ind} on temperature was used to estimate the activation energy for gypsum crystallization. Subsequently, the same measurement technique was applied to study the effect of calcium and sodium chloride salts on the calcium sulfate dihydrate induction period (Prisciandaro et al., 1999), showing that Cl^- ions have a strong effect on gypsum precipitation by retarding nucleation kinetics. The intensity of this effect depended on the kind ($CaCl_2 \cdot 2H_2O$ or NaCl) and the concentration of salt added in solution to increase chlorine concentration with respect to equimolar conditions.

The purpose of the present article is to report the evaluation of the activation energy and the interfacial tension for gypsum nucleation in a solution containing a fixed amount of sodium chloride. Such values are also compared with those previously obtained (Lanica et al., 1999), when the NaCl dissolved into the gypsum mother liquor was exclusively caused by the presence of Na^+ and Cl^- ions in the feed solution salts.

Experimental Apparatus and Procedure

The experimental apparatus consists of a stirred reactor with a related optical device, and is shown in Figure 1. The reactor is a batch cylindrical crystallizer, made of glass, with a working volume of 1.0×10^{-3} m^3 and diameter of 0.09 m. The crystallizer is surrounded by a water jacket for temperature control; stirring is provided by a two-blade polypropylene stirrer, with rotation rate ranging between 1 and 10 s^{-1}. An offtake tube, placed at half of the working height of the vessel, allows the removal of samples of the suspension; the position of the tube has been chosen to ensure that the content of the exit stream is the same as the content of the reactor (Zacek et al., 1982).

The stream removed by the offtake tube is sent by a peristaltic pump to an analysis flowthrough cell, and then is conveyed again to the crystallizer. The cell, made of quartz, is 0.07 m long, with a square section of 0.01 m and 0.0025 m thickness. A 10-m W He−Ne laser beam ($I_0 = 632.8$ nm) is focused on the cell, orthogonal to its walls; the beam is vertically polarized with a diameter of 2 mm. On the path of the laser, placed at 45° with respect to beam direction, a beam splitter is provided in order to divide the laser beam into two parts: one to illuminate the measure cell, while the other, collected by a photodiode, to check the stability and intensity of laser beam (I_o). The signal of the scattered light (I_{sca}) is collected by two lenses of focal 120 and 50 mm, at 90° with respect to the laser beam; this signal is sent, through a quartz optical fiber that ends on an interferential filter, to a photomultiplier tube, connected to a power supply with voltage that is variable in the 0−1000 V range. The signal of the transmitted light (I_{trans}) is collected by a photodiode located beyond the cell, at 0° with respect to the laser beam. The two analog signals of scattered and transmitted light, together with I_o, are collected by a recorder device (Prisciandaro, 1998).

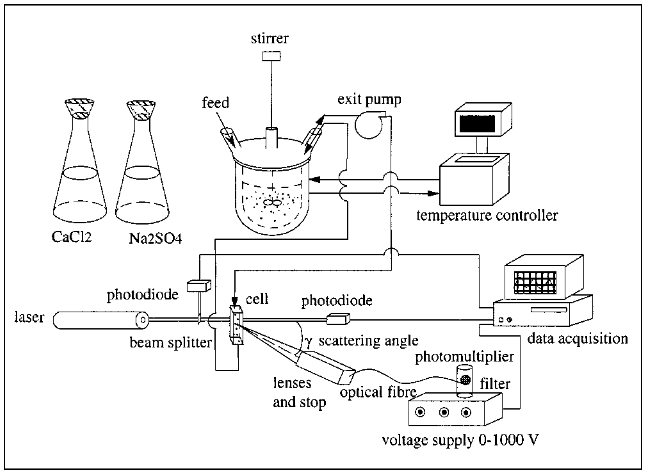

Figure 1. Experimental apparatus.

Supersaturated solutions of calcium sulfate were prepared by using two clear aqueous solutions of reagent-grade $CaCl_2 \cdot 2H_2O$ and Na_2SO_4 in bidistilled water. The dissolved Ca^{2+} ion concentration was measured by EDTA titration using Idranal Pellets (Riedel-de Haen) as an indicator, while SO_4^{2-} ion concentration was measured by means of turbidity measurements carried out in a spectrophotometer (Hach, DREL/5). After their preparation the two solutions were filtered by using a 0.22-μm filter (Millipore) and a vacuum pump, in order to eliminate all foreign material inevitably present in the solution, and then mixed directly into the reactor. The concentration of $CaCl_2 \cdot 2H_2O$ and Na_2SO_4 varied between 38 mol/m^3 and 94 mol/m^3. Excess of chlorine ion with respect to the equimolar feed was obtained by adding an amount of NaCl, whose concentration in the reactor solution varied between 19 and 60 mol/m^3, therefore the concentration of Cl^- ranged from 57 mol/m^3 to 180 mol/m^3.

The supersaturation was calculated considering the following liquid−solid equilibrium between Ca^{2+} and SO_4^{2-} ions and solid $CaSO_4 \cdot 2H_2O$:

$$Ca^{2+} + SO_4^{2-} + 2H_2O = CaSO_4 \cdot 2H_2O \tag{1}$$

so that it is

$$\sigma = \frac{a_{Ca^{2+}} a_{SO_4^{2-}} a_w^2}{K_{ps}}, \tag{2}$$

where a_I is the activity expressed as the product of the molality (m_I) and the activity coefficient (γ_I) of the I species (I = Ca^{2+}, $SO_4^{\ 2-}$, and water), and K_{ps} is the solubility product of gypsum. The value of K_{ps} was calculated as a function of temperature by means of the following relationship:

$$\ln\left(K_{ps}\right) = 390.9619 - 152.6246 \log T - 12545.62/T + 0.0818493T \quad (3)$$

obtained by Marshall and Slusher (1966) for calcium sulfate dihydrate in aqueous sodium chloride solutions from 0°C to 110°C (see also Barba et al., 1982; and Budz et al., 1986). The activity coefficient calculations in the supersaturated solution were performed by using the Bromley (1973) approach and are reported in a previous work (Lancia et al., 1999).

The excess of Cl^- ions has been defined as follows:

$$E = \frac{\left[Cl^-\right] - \left[Cl^-_{eqm}\right]}{\left[Cl^-_{eqm}\right]}, \quad (4)$$

where Cl^- is the molar concentration of chlorine in solution, and Cl^-_{eqm} is the chlorine introduced in solution through the equimolar feed as $CaCl_2 \cdot 2H_2O$.

All experiments have been carried out for a fixed value of chlorine excess, namely $E = 0.5$. Supersaturation was varied in the 2–4 range and four temperature levels were explored, specifically 25, 35, 50 and 70°C.

The induction period was evaluated by measuring the intensity of scattered and transmitted light as a function of time and by adopting two parallel procedures, one graphical and the other one numerical, as described in detail elsewhere (Lancia et al., 1999), which gave quite similar (±10%) results.

Results and Discussion

In Figures 2 and 3 the smoothed curves of I_{sca}/I_0 and I_{trans}/I_0 are reported as a function of time for $T = 25$°C and for two different values of supersaturations (σ = 2.4 and 2.6); in particular, Figure 2 refers to stoichiometric conditions (E = 0), while Figure 3 refers to a condition in which an excess of chlorine ions has been added in the solution as NaCl ($c_{NaCl} = 56$ mol/m^3, curves C; $c_{NaCl} = 50$ mol/m^3, curves D), for which $E = 0.5$. Figures 2 and 3 show the strong influence exerted by supersaturation on the induction period (see Mullin, 1993). The comparison among curves in Figure 2 and those in Figure 3 shows well that when a chlorine excess is present in solution (Figure 3), with respect to equimolar conditions, it inhibits gypsum nucleation kinetics with respect to the case of $E = 0$ (Figure 2) (Lancia et al., 1999).

In Figure 4 the smoothed curves of I_{sca}/I_0 and I_{trans}/I_0 are reported as a function of time for $\sigma = 2.6$, $E = 0.5$, and for three different temperature values ($T = 25$, 50 and 70°C). These figures clearly show the strong effect of temperature on the induction period, which decreases as the temperature increases.

Figure 5 reports the logarithm of t_{ind} vs. $1/T$ for three different levels of supersaturation ($E = 0.5$; σ = 2.4, 2.6, 3.0). The linear relationship existing between the logarithm of t_{ind} and the inverse of the absolute temperature, already found in the case of $E = 0$ (Lancia et al., 1999) and reported in Figure 5 (dotted line), still remains. However, the slope of the straight lines is higher when $E = 0.5$, suggesting that when a chlorine excess is present in the solution, the effect of T on t_{ind} is stronger than in the case of equimolarity (Lancia et al., 1999).

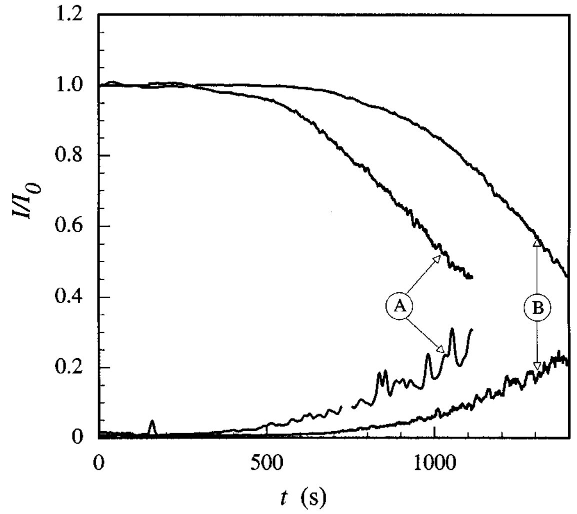

Figure 2. Intensities of the scattered (I_{sca}) and transmitted (I_{trans}) light as a function of time for different values of supersaturation.

T = 25°C, E = 0, no additives; A curves; σ = 2.6, B curves: σ = 2.4.

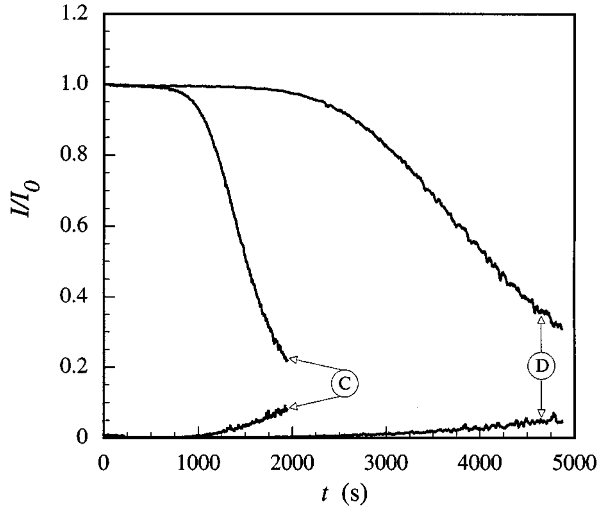

Figure 3. Intensities of the scattered (I_{sca}) and transmitted (I_{trans}) light as a function of time for different values of supersaturation.

T = 25°C, E = 0.5; C curves: c_{NaCl} = 56 mol/m^3, σ = 2.6; D curves: c_{NaCl} = 50 mol/m^3, σ = 2.4.

Figure 6 shows the dependence of the induction period on supersaturation for three temperature levels—that is, 25, 50 and 70°C—for $E = 0.5$. It can be observed that the induction period for gypsum nucleation continuously decreases with increasing supersaturation. By using the following semiempiri-

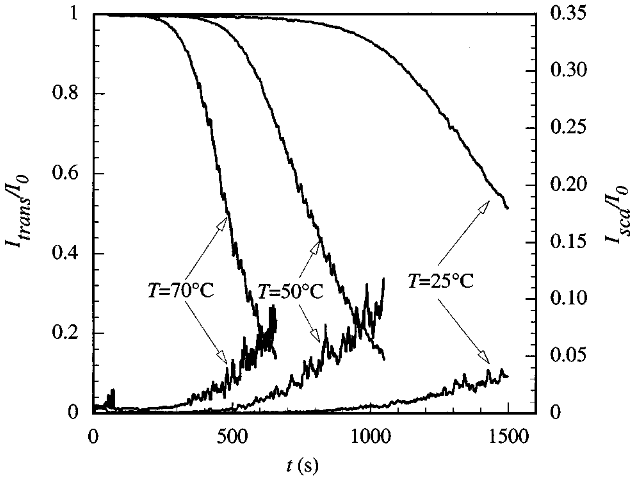

Figure 4. Intensities of the scattered (I_{sca}) and transmitted (I_{trans}) light as a function of time for different values of temperature.

$\sigma = 2.6$, $E = 0.5$.

cal correlation to correlate experimental data (Packter, 1974),

$$t_{ind} = \frac{K}{\sigma^r}, \tag{5}$$

where K and r are empirical constants, the curves sketched in Figure 6 are obtained. In particular, a nonlinear regression analysis gives $K = 1.1 \times 10^5$, 5.1×10^4 and 3.8×10^4 s for $T =$ 25, 50 and 70°C, respectively; while r is almost independent of temperature and equal to 5.0 A similar behavior was previously obtained for the case of $E = 0$ by Lancia et al. (1999).

Experimental data of the induction period plotted as a function of supersaturation levels can be adequately used, as suggested by Söhnel and Garside (1992), to distinguish between homogeneous and heterogeneous nucleation phenomena. This is worth noting in the estimation of some characteristic parameters of primary nucleation, such as the activation energy and the interfacial tension.

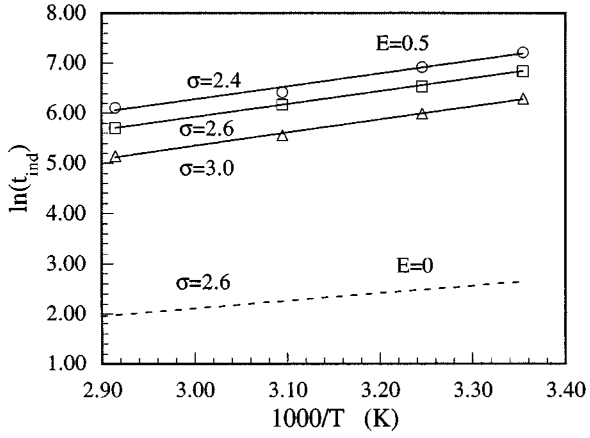

Figure 5. Dependence of the induction period on the inverse of temperature.

$E = 0.5$; ○: $\sigma = 2.4$; □: $\sigma = 2.6$; Δ: $\sigma = 3.0$.

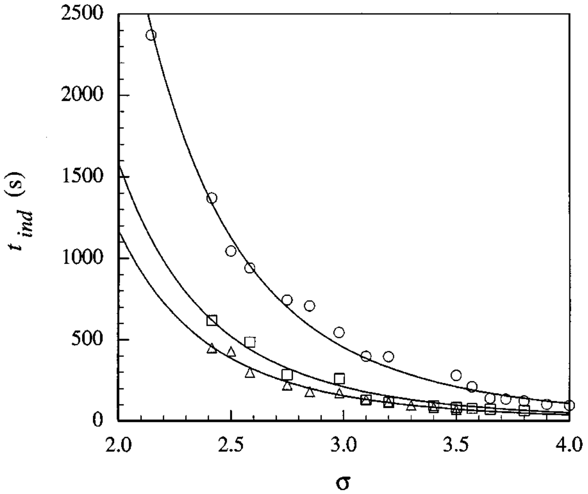

Figure 6. Induction period as a function of supersaturation.

$E = 0.5$; ○: $T = 25°C$; □: $T = 50°C$; Δ: $T = 70°C$.

For this purpose or aim, the following equation derived from homogeneous nucleation equations, was considered (He et al., 1994):

$$\log(t_{ind}) = A_1 + \frac{A_2}{T^3(\log \sigma)^2}, \tag{6}$$

where A_1 is an empirical constant and A_2 is given by

$$A_2 = \frac{\eta \gamma_s^3 \mu^2 N_A f}{(2.3R)^3}, \tag{7}$$

in which η is a shape factor, γ_S is the surface energy, N_A is the Avogadro number, R is the gas constant, μ the molecular volume, and f is a correction factor that takes into account the heterogeneous nucleation; in particular, according to Söhnel and Mullin (1988), when purely homogeneous nucleation takes place, it is $f = 1$, while when heterogeneous nucleation occurs, it is $f < 1$. Consequently, a change in the slope of the experimental results could indicate a transition from homogeneous to heterogeneous nucleation mechanisms. In Figure 7a, 7b, 7c, the distinction between the two nucleation mechanisms is reported for the temperatures T = 25°C, 50°C, and 70°C. In Figure 7a, the passage from homogeneous to heterogeneous nucleation is quite visible, and following the approach of Söhnel and Garside (1992), the experimental data in the middle part of the plot have not been taken into account in the interpolation of the experimental results, but are considered to belong to a "transition zone."

In order to gain values relative to the homogeneous nucleation region solely, experiments at higher temperature ($T =$ 50 and 70°C) have been carried out for a very high value of supersaturation (such as for very low values of $1/(\log \sigma)^2$). In particular, considering the influence of temperature on the induction period (see Figure 4), at a high temperature the

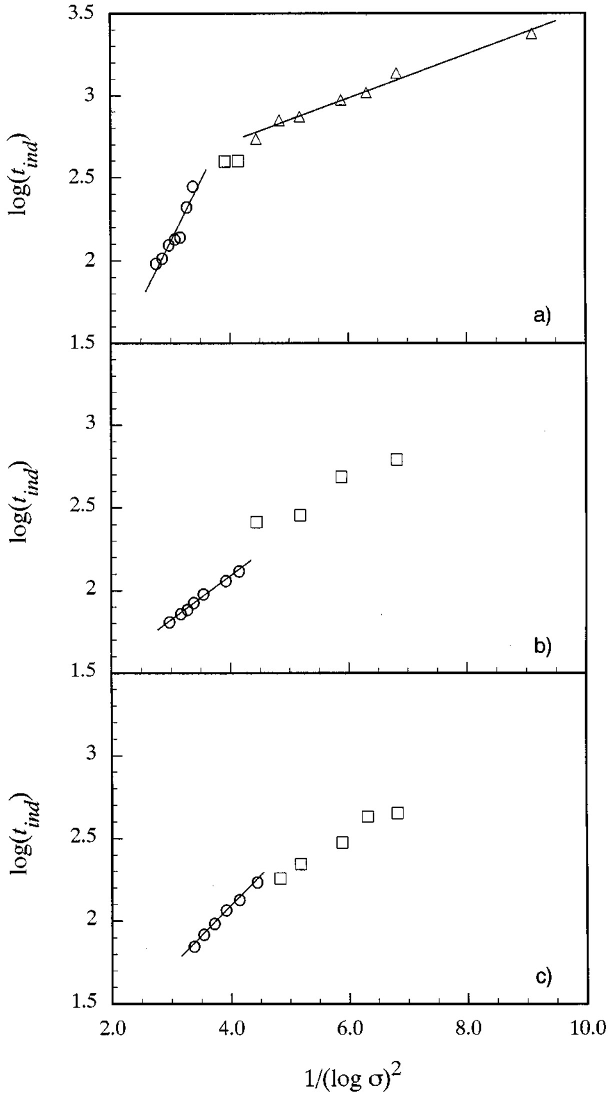

Figure 7. Induction period as a function of supersaturation.

$E = 0.5$; (a) $T = 25°C$; (b) $T = 50°C$; (c) $T = 70°C$; ○: homogeneous nucleation; □: transition zone; Δ: heterogeneous nucleation.

passage from homogeneous to heterogeneous nucleation mechanism takes place at low values of σ (that is, at the high value of $1/(\log \sigma)^2$), therefore in the plot $\log(t_{ind})$ vs. $1/(\log \sigma)^2$, the transition region moves toward the right. For this reason, a supersaturation level higher than 3 (that is, $1/(\log \sigma)^2 < 4.5$) appeared sufficient to restrict the experimental results to the desired homogeneous region. Figure 7b and 7c show experimental results relative to $T = 50$ and 70°C, respectively; in these figures it is possible to recognize the homogeneous region, as well as some experimental data belonging to the transition region toward the heterogeneous nucleation mechanism.

Once the distinction between homogeneous and heterogeneous nucleation data have been made, the estimation of the activation energy for the primary nucleation of gypsum and the interfacial tension between the gypsum crystals and the surrounding aqueous solution can be easily performed. The following empirical relationship, proposed by Liu and Nancollas (1975), was used to correlate data of t_{ind} vs. T:

$$t_{ind} = \tau \exp\left(\frac{E_{att}}{RT}\right), \tag{8}$$

where τ is a constant, E_{att} is the activation energy for the process, and R is the gas constant. In particular, Eq. 8 was reported as continuous lines in Figure 5, and from the slopes of these straight lines the value of 49.7 kJ/mol was determined for the activation energy. This value is higher than that previously found ($E_{att} = 30$ kJ/mol; Lancia et al., 1999), leading to a slower nucleation kinetic.

As regards the interfacial tension values, from the slopes of the straight lines reported in Figure 7a, 7b, 7c, relative to the homogeneous nucleation region, the average value of 37.8 mJ/m^2 was evaluated [in Eq. (7) it was considered that $\eta = 16\pi/3$, assuming spherical particles, and $\mu = 74.69$ cm^3/mol]. The comparison among the interfacial tension values obtained for different temperature levels in the presence ($\gamma_s = 37.8$ mJ/m^2) and in the absence of excessive chlorine ($\gamma_s = 36.8$ mJ/m^2), indicates that the interfacial tension between gypsum crystals and the aqueous solution is not influenced by the presence of NaCl.

Conclusions

The induction period for gypsum nucleation has been experimentally measured by using an optical technique for a supersaturation ranging from 2 to 4, a temperature varying between 25 and 70°C, and with a chlorine excess E, added as NaCl, that is equal to 0.5. Activation energy for gypsum crystallization and the interfacial tension between gypsum crystals and the aqueous solution have been calculated by means of the experimental measurements of induction time. These values have been compared with those previously estimated in the absence of a chlorine excess, and the following conclusions have been reached:

- The temperature has a strong accelerating effect on gypsum nucleation kinetics, by reducing the induction period values, and this effect is stronger when $E = 0.5$ with respect to the case of $E = 0$;
- The supersaturation is indeed able to accelerate the precipitation phenomenon, and the intensity of its effect is higher at low temperature;
- The effect of NaCl on the induction period is more marked at low temperature values than at high temperatures;
- The delay of the primary nucleation of gypsum in the presence of a chlorine excess is confirmed by the activation energy value, which is higher when $E = 0.5$ (49.7 kJ/mol) with respect to the case of $E = 0$ (30 kJ/mol);
- The interfacial tensions between crystal and solution is of 37.8 mJ/m^2, which does not vary significantly in the temperature interval explored, and that is not influenced by the presence of NaCl in solution.

Notation

a = activity, mol/m^3
A_1 = constant in Eq. 6, dimensionless

A_2 = constant in Eq. 6, K^3
c = concentration, mol/m^3
E = chlorine excess as defined by Eq. 4, dimensionless
E_{att} = activation energy, J/mol
f = correction factor in Eq. 7, dimensionless
I = intensity of light, W/m^2
K = constant in Eq. 5, s
K_{ps} = solubility product, mol^4/kg^4
N_A = Avogadro number, mol^{-1}
r = constant in Eq. 5, dimensionless
R = gas constant, J/mol K
t = time, s
t_{ind} = induction period, s
t^* = true induction period, s
T = absolute temperature, K
V = volume, m^3

Greek letters

γ = activity coefficient, dimensionless
γ_s = surface energy, J/m^2
η = shape factor, dimensionless
λ_0 = wavelength, m
μ = molecular volume, m^3/mol
σ = supersaturation, dimensionless
τ = constant in Eq. 8, s

Subscripts

abs = absorption
eqm = equimolar
sca = scattering
trans = transmitted
w = water
0 = relative to incident light

Literature Cited

Amjad, A. B., and J. Hooley, "Influence of Polyelectrolytes on the Crystal Growth of Calcium Sulphate Dihydrate," *J. Colloid Interface Sci.*, 111, 496 (1986).

Barba, D., V. Brandani, and G. Di Giacomo, "A Thermodynamic Model of CaSO$_4$ Solubility in Multicomponent Aqueous Solutions," *Chem. Eng. J.*, **24**, 191 (1982).

Bromley, L. A., "Thermodynamic Properties of Strong Electrolytes in Aqueous Solutions," *AIChE J.*, **19**, 313 (1973).

Budz, J., A. G. Jones, and J. W. Mullin, "Effect of Selected Impurities on the Continuous Precipitation of Calcium Sulphate (Gypsum)," *J. Chem. Tech. Biotechnol.*, **36**, 153 (1986).

Etherton, D. L., and A. D. Randolph, "Nucleation/Growth Rate Kinetics of Gypsum in Simulated FGD Liquors: Some Process Configurations for Increasing Particle Size," *AIChE Symp. Ser.*, **77**, 87 (1981).

He, S., J. E. Oddo, and M. B. Tomson, "The Nucleation Kinetics of Calcium Sulfate Dihydrate in NaCl Solutions up to 6 m and 90°C," *J. Colloid Interface Sci.*, **162**, 297 (1994).

Lancia, A., D. Musmarra, and M. Prisciandaro, "Measurement of the Induction Period for Calcium Sulfate Dihydrate Precipitation," *AIChE J.*, **45**, 390 (1999).

Liu, S. T., and G. H. Nancollas, "A Kinetic and Morphological Study of the Seeded Growth of Calcium Sulfate Dihydrate in the Presence of Additives," *J. Colloid Interface Sci.*, **52**, 593 (1975).

Marshall, W. L., and R. Slusher, "Thermodynamics of Calcium Sulfate Dihydrate in Aqueous Sodium Chloride Solutions, 0−110°," *J. Phys. Chem.*, **70**, 4015 (1966).

Mullin, J. W., *Crystallization*, 3rd ed., Butterworth-Heinemann, Oxford (1993).

Nielsen, A. E., *Kinetics of Precipitation*, Pergamon Press, Oxford (1964).

Öner, M., Ö. Dogan, and G. Öner, "The Influence of Polyeletrolytes Architecture on Calcium Sulfate Dihydrate Growth Retardation," *J. Cryst. Growth*, **186**, 427 (1998).

Packter, A., "The Precipitation of Calcium Sulphate Dihydrate from Aqueous Solution—Induction Period, Crystal Numbers and Final Size," *J. Cryst. Growth*, **21**, 191 (1974).

Prisciandaro, M., "Crystallizzazione del Solfato di Calcio Biidrato nel Processo di Desolforazion ad Umido dei Fumi della Combustione," PhD Diss. Univ. of Naples "Federico II," Naples, Italy (1998).

Prisciandaro, M., A. Lancia, and D., Musmarra, "The Influence of Typical FGD Impurities on Gypsum Nucleation," *Proc. Symp. on Industrial Crystallization*, Cambridge, UK (1999).

Söhnel, O., and J. Garside, *Precipitation*, Butterworth-Heinemann, Oxford (1992).

Söhnel, O., and J. W., Mullin, "A Method for the Determination of Precipitation Induction Periods," *J. Cryst. Growth*, **44**, 377 (1978).

Söhnel, O., and J. W. Mullin, "Interpretation of Crystallization Induction Periods," *J. Colloid Interface Sci.*, **123**, 43 (1988).

Zacek, S., J. Nyvlt, J. Garside, and A. W. Nienow, "A Stirred Tank for Continuous Crystallization Studies," *Chem. Eng. J.*, **23**, 111 (1982).

Manuscript received Dec. 8, 1999, and revision received Aug. 8, 2000.